

# miR-638 suppresses cervical cancer progression by inhibiting *NCAPG2* under the treatment of Tetrandrine

Min Wang<sup>1\*</sup>, Kai Liu<sup>2\*</sup>, Zhongming Zhou<sup>1</sup> and Huizhuan Geng<sup>3</sup>

<sup>1</sup>Department of Gynecology, <sup>2</sup>Department of Nuclear Medicine, Hubei Provincial Hospital of Traditional Chinese Medicine and <sup>3</sup>Department of Gynecology, First Clinical College, Hubei University of Chinese Medicine, Wuhan, Hubei, PR China

\*These authors contributed equally to this work

**Summary.** Background. The interaction of microRNA with Chinese herbal medicines is a promising therapeutic approach for prevention of cervical cancer.

Methods. Western blotting or qRT-PCR were carried out to identify the expression of *NCAPG2* and miR-638. A tetrandrine (TET) cell model was used to explore the effects of miR-638 and its target gene *NCAPG2* using CCK-8, transwell, wound healing, and western blot assays. Furthermore, luciferase activity assay was conducted to measure the interaction among TET, *NCAPG2* and miR-638.

Results. Under TET treatment, Hela and SiHa cells exhibited repressed cell viability, migration, invasion, and epithelial-mesenchymal transition (EMT), and these effects were further enhanced by high expression of miR-638. In contrast, *NCAPG2* expression was low in TET-treated cells and had an opposite effect to that of miR-638.

Conclusion. We highlighted that miR-638 suppresses cervical cancer progression by inhibiting *NCAPG2* under tetrandrine treatment.

**Key words:** miR-638, *NCAPG2*, Tetrandrine, Cervical cancer

## Introduction

Cervical carcinoma originates from cervical intraepithelial lesions, where high-risk human papillomavirus (HPV) infection acts as a major facilitator, along with additional genetic and epigenetic changes in the pathogenetic process (Burd, 2003; Olusola et al., 2019). Up-to-date studies concerning

cervical cancer highlight that those epigenetic changes are prevalent in the occurrence and metastasis of this disease (Fang et al., 2014; Laengsri et al., 2018). Researchers have uncovered new information on non-coding RNAs, particularly long non-coding RNAs (lncRNAs) and microRNAs (miRNAs), and there is rising interest in using these factors as biomarkers for disease diagnosis and therapy (Park et al., 2017; Pardini et al., 2018; Sun et al., 2019; Sadri Nahand et al., 2020). However, our knowledge of the role and utility of miRNAs in the pathogenesis of cervical cancer is limited. Therefore, we tried to expand our current understanding with the hope that it will reduce the unfavorable outcomes of cervical cancer.

MiR-638 is of particular interest as it has been described as a distinct tumor suppressor in various carcinoma processes, such as glioma (Zheng et al., 2018), gastric carcinoma (Zhang et al., 2015) and Ewing sarcoma (Zhou et al., 2018). Specifically, it has also been reported to suppress cancers in cervical cancer, but as far as we know, there are only two of these reports (Wei et al., 2017; Zheng et al., 2020), a listing demonstrates the miR-638 function in cervical cancer. They elucidated the cancer-suppressive function of miR-638, which was considered a reason for our investigation of the detailed role of miR-638 in cervical cancer.

It is generally acknowledged that miRNAs contribute in various biological processes, including cervical cancer progression, by interfering directly with messenger RNA (mRNA) and inhibiting target gene expression (Wilting et al., 2010; Shishodia et al., 2015; Mori et al., 2019). TargetScan predicted that non-SMC condensin II complex subunit G2 (*NCAPG2*) was a target gene of miR-638. This gene belongs to the complex of chromosome condensin II and plays an important function in the condensation and segregation of chromosomes during mitosis (Khan et al., 2019). It is noteworthy that this biological process is important for appropriate bi-oriented chromosome separation (Thadani et al., 2012), while abnormal processes may lead to

Corresponding Author: Huizhuan Geng, Department of Gynecology, First Clinical College, Hubei University of Traditional Chinese Medicine, No. 16 Huangjiahu West Road, Hongshan District, Wuhan 430065, Hubei, PR China. e-mail: huizhuangeng@163.com  
www.hh.um.es. DOI: 10.14670/HH-18-657



tumorigenesis. NCAPG2, being a critical regulator of this pathway, also has a role in tumorigenesis (Zhan et al., 2017; Meng et al., 2019). Based on these reports, we aimed to investigate the interaction among miR-638 and NCAPG2 in cervical cancer.

Tetrandrine (TET) is an active ingredient isolated from the herbal plant *Stephania tetrandra*, which has been traditionally and historically exploited as antipyretic and an anti-inflammatory in medicine in China (Kwan and Achike, 2002; Bhagya and Chandrashekar, 2018). Over the past few decades, TET has gained considerable attention because of its cardiovascular electrophysiological properties as a Ca<sup>2+</sup> antagonist (Rao, 2002; Yao and Jiang, 2002; Zhang et al., 2017). More recently, it was discovered that in addition to this distinct effect, TET can be potentially used as an anti-tumor agent or as an adjunct to chemotherapy and radiotherapy (Chen, 2002; Chow et al., 2019; Liao et al., 2019). It has been demonstrated that TET possesses cytotoxicity and antibacterial activity, and meets the structural requirements of anti-tumor activity up to a point (Kuroda et al., 1976). We focused on TET's tumor-related role in cervical cancer in this study, hypothesizing that TET may be exploited as a powerful anti-tumor drug in cervical cancer treatment.

To further elucidate the regulatory role of miR-638 in cervical cancer, we aimed to comprehensively demonstrate its action on TET-treated cervical cancer cell lines. We then confirmed NCAPG2 as a miR-638 target gene in the regulation of cervical cancer cells. Overall, the control of NCAPG2 by miR-638 might constitute a new regulatory axis in the advancement of cervical cancer.

## Materials and methods

### Cell lines

ATCC (USA) provided the human cervical cancer cell lines HeLa and SiHa, which were maintained at 37°C and 5% CO<sub>2</sub> in DMEM with 10% FBS (Gibco, USA) and 1% penicillin and streptomycin. The TET cell model was established by assessing suitable concentrations and time points for TET in SiHa and HeLa cells using the CCK-8 assay. Time points were 0, 24, 48, 72, and TET concentration was 0, 1, 3, 10, and 30 μM.

### Cell transfection

GenePharma (Shanghai, China) provided overexpressing NCAPG2 (OE-NCAPG2) and empty vector (OE-NC) plasmids. Briefly, the full length of NCAPG2 was amplified and then subcloned in the vector (pcDNA3.1) to obtain the NCAPG2 overexpression plasmid (OE-NCAPG2), and pcDNA3.1 empty vector was used as the negative control for OE-NCAPG2. MiR-638 mimics and corresponding negative controls (miR-NC) used for transfection were purchased from GenePharma (Shanghai, China). Transfection was performed by

Lipofectamine 3000 from Invitrogen, USA.

### Quantitative real-time polymerase chain reaction (qRT-PCR)

With the help of the TRIzol reagent (Invitrogen), total RNA was extracted. The PrimeScript reverse transcription reagent kit and the genomic DNA (gDNA) Eraser kit from Takara, Japan were employed to reverse transcribe RNA into cDNA for NCAPG2. Using the miDETECT A Track miRNA RT-qPCR Starter Kit, (RiboBio, China) RNA was reverse transcribed into cDNA for miR-638. qRT-PCR was executed by means of TB Green Premix Ex Taq II (Takara, Japan) on an ABI 7300 Real-time PCR system (Applied Biosystems, USA) using the primer sequences listed in Table 1. *U6* and *GAPDH* were applied as the internal controls. We applied 2<sup>-ΔΔCt</sup> method for calculation of the relative expression levels.

### CCK-8

We used Cell Counting Kit-8 (Dojindo, Japan) and followed the instructions on this kit to ascertain cell viability. SiHa and HeLa cells were maintained at a concentration of 1,000 cells per well in 96-well plates. At appropriate transfection times of 0, 24, 48, and 72 hours, 10 μL CCK-8 solution was added to the well to continue incubation. Optical density was assessed using a microplate reader at 450 nm (Synergy 4, USA).

### Wound healing assay

The cell monolayer was scraped using a sterile 200 μL pipette tip and then cultured in serum-free medium. In five random areas in each sample, the wound was inspected and photographed using an Olympus inverted microscope immediately and 48 hours after scratching. The cell migration rate was calculated as: Mobility (%) = 1 - (24-h scratch distance/initial distance) × 100%.

### Transwell invasion assay

Cell invasion was verified by a transwell assay using a transwell chamber coated with Matrigel (Corning

**Table 1.** The sequences of PCR primers in this study.

Primer	Sequences
NCAPG2	Forward: 5'-AGACAGGAAGAAGACTGGCG-3' Reverse: 5'-GTTCCGTAGTGCCCGGTAG-3'
miR-638	Forward: 5'-TAGGCAGGATGGCACTGGGAGC-3' Reverse: 5'-GTGTGATTCCACAGAGGCCAGA-3'
GAPDH	Forward: 5'-GAGTCAACGGATTTGGTCGTA-3' Reverse: 5'-TTCCCGTTCTCAGCCTTGAC-3'
U6	Forward: 5'-AACGCTTACGAATTTGCGT-3' Reverse: 5'-CTCGCTTCGGCAGCAC-3'

## miR-638 suppresses cervical cancer progression

Incorporation, USA). In brief, after 48h of transfection, 200  $\mu$ L of serum-free DMEM medium was used to resuspend the collected cells ( $1 \times 10^4$ ). The cells were then put in the upper chamber and incubated for 24 hours at 37°C. At the same time, 600  $\mu$ L of complete DMEM medium was added to the lower chamber. After incubation, the cells that passed through the top chamber to the lower chamber were fixed with methanol. The non-traversed cells that remained in the upper chamber were swabbed with cotton swabs. Following fixation, the traversed cells in the lower chamber were stained with crystal violet. The cells were then counted under a microscope (Leica, Germany).

### Cell cycle assay

LNCaP and 22RV1 cells ( $1 \times 10^6$  cells) after transfection for 72h were collected and centrifuged, washed twice with phosphate-buffered saline (PBS) and precipitated. The precipitates were fixed in 70% ethanol at 4°C for 4h. Next, the cells were stained with 500  $\mu$ L of staining solution (staining buffer 465  $\mu$ L, 50 $\times$  RNase A 10  $\mu$ L, 20 $\times$  propidium iodide 25  $\mu$ L) at 37°C for 1h according to Beyotime Cell Cycle (shanghai, China) manufacturer's instructions. Finally, the cell cycle distribution was uncovered utilizing flow cytometry (FACS Canto™ II Flow Cytometer, BD Biosciences, USA).

### Bioinformatics analysis

GSE30656 (Wilting et al., 2013) from GEO DataSets is an miRNA microarray that includes miRNA expression of cervical cancer and normal non-tumor samples. The downregulated miRNAs in cervical cancer samples were screened with  $\log_{2}FC \leq -1.5$  and adjusted  $P < 0.05$ . TargetScan was employed for prediction of the target genes (Agarwal et al., 2015). GSE63514 (den Boon et al., 2015) from GEO DataSets and GEPIA, including mRNA expression in cervical cancer and normal non-tumor samples, was used to screen the upregulated mRNAs in cervical cancer samples with  $\log_{2}FC \geq 2$  and adjusted  $P < 0.05$ . By intersecting the two datasets (GSE63514 and GEPIA) with the targets predicted by TargetScan, we obtained seven genes that overlapped and uploaded them to STRING for protein-protein interaction analysis.

### Luciferase assay

The binding site was predicted at position 2071-2076 of the 3'-UTR of *NCAPG2* mRNA by TargetScan. The predicted or mutant ("GAUCCC" modified to "ACGTTT") miR-638 target sequences from the 3'-UTR of *NCAPG2* mRNA were cloned into the pMIR-Report luciferase vector (Promega, USA). One day before co-transfection, cells ( $1.5 \times 10^5$ ) were seeded in duplicates onto 12-well plates with miR-638 mimics or miRNA mimic negative control at a final concentration of 50 nM, along with 1 ng of *NCAPG2* WT or *NCAPG2*

MUT. The dual luciferase detector assay system (Promega) was employed to assess the activity of Firefly and Renilla luciferases after 48 hours transfection

### Western blotting

Total protein was extracted using RIPA buffer from Sigma-Aldrich, USA. Twenty micrograms of protein was subjected to sodium dodecyl sulfate-polyacrylamide gel electrophoresis. The samples were transferred to polyvinylidene fluoride membranes, and the proteins were blocked with 5 percent nonfat milk for 2 hours. Then, the membranes were incubated with anti-NCAPG2 (1:1000; cat#: ab70350, Abcam, UK), anti-E-cadherin (1:1000; cat#: ab238099, Abcam), and anti-N-cadherin (1:1000; cat#: ab76011, Abcam). Anti-GAPDH (1:1000; cat#: ab9485, Abcam) was used as the loading control. After overnight incubation at 4°C, the membrane was incubated at room temperature and incubated for two hours with secondary antibodies. After washing with TBST, ECL (Thermo Fisher Scientific, USA) was used to detect the protein bands. Finally, the optical densities of the bands were calculated using software ImageJ.

### Data analysis

For statistical analysis, the SPSS 19.0 (USA) was utilized. All of the investigations were carried out in triplicate, and the results are presented as the mean  $\pm$  standard deviation (SD). To compare differences between two groups, the Student's t-test was utilized. A one-way analysis of variance was used to examine differences across several groups (ANOVA). Statistical significance was set at  $P < 0.05$ .

## Results

### TET might restrain cervical cancer development *in vitro*

The chemical structure of TET is shown in Fig. 1A. From Figure 1B, it can be observed that TET influenced the viability of HeLa and SiHa cells in a dose- and time-dependent manner. Specifically, cell viability declined to approximately 50% when challenged with 10  $\mu$ M TET for 48h. Hence, 10  $\mu$ M TET was used in the subsequent *in vitro* experiments. Cell migration of HeLa and SiHa cells was significantly repressed by 40 and 55%, respectively, when the cells were treated with 10  $\mu$ M TET (Fig. 1C). Besides, TET treatment also had a great inhibitory effect on the invasion of HeLa and SiHa cells (Fig. 1D), with approximately 30% inhibition in HeLa cells and approximately 40% inhibition in SiHa cells. Moreover, epithelial-mesenchymal transition (EMT)-related proteins, E-cadherin and N-cadherin, were measured to evaluate the variation of EMT in cervical cancer cells treated with TET. Western blot analysis showed that E-cadherin was enhanced by 1.4 and 1.7 times and N-cadherin was reduced to 0.7 and 0.5 in

HeLa and SiHa cells, respectively, in comparison with the DMSO-treated group (Fig. 1E). In addition, EMT treatment enhanced G0/G1 phase cells proportion and decreased S phase cell proportion in flow cytometry analysis (Fig. 2). These findings suggest that TET may restrain cervical cancer progression *in vitro*.

*miR-638 and NCAPG2 might affect cervical cancer development*

By profiling GSE30656, six miRNAs were identified to be significantly downregulated in cervical cancer, hsa-miR-370, hsa-miR-203, hsa-miR-494, hsa-

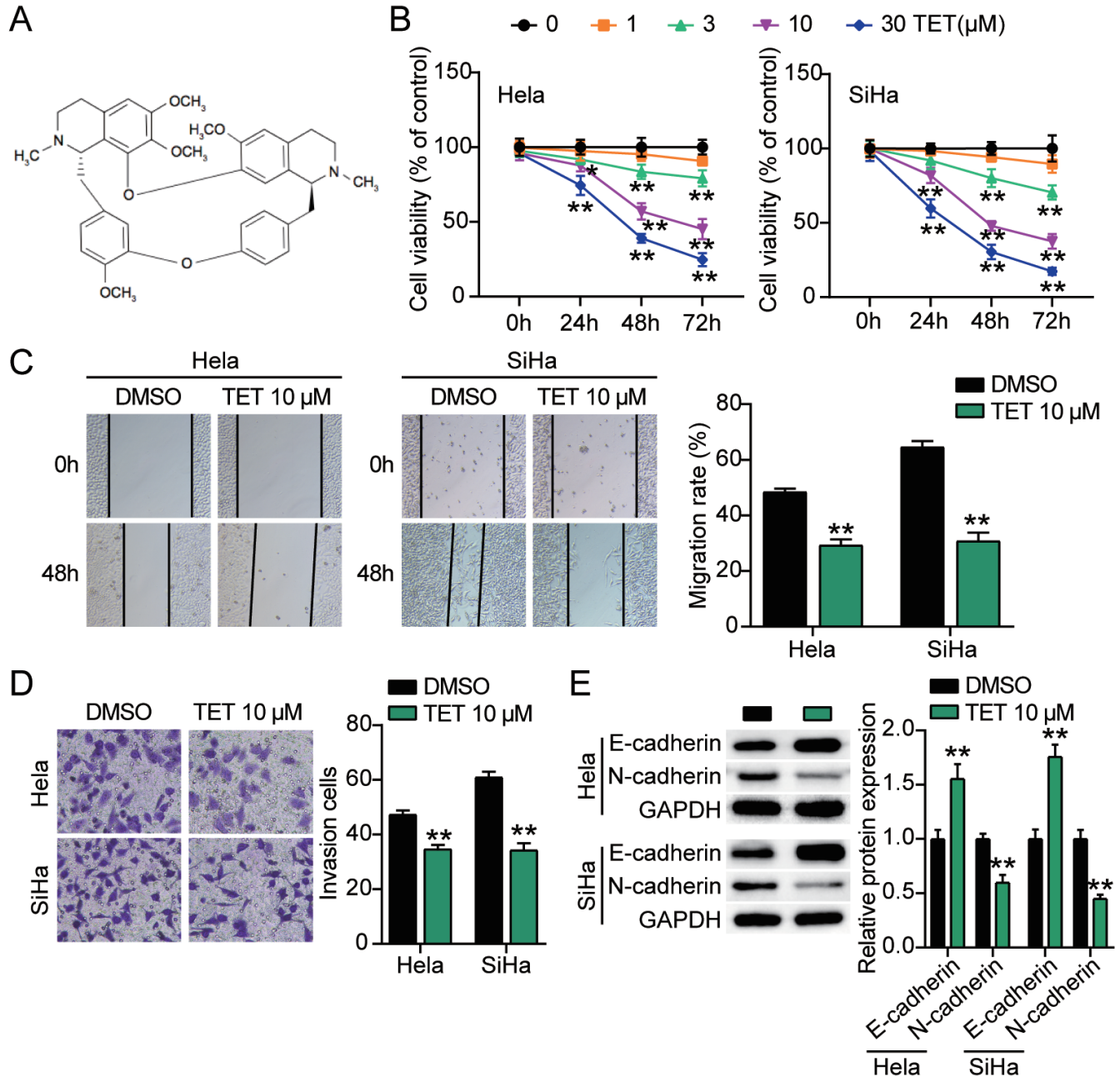


**Fig. 1.** TET possessed cancer-prevention ability in cervical cancer. **A.** The molecular structure of Tetrandrine. **B.** The cell viability of HeLa and SiHa was inhibited by 10 μM of TET, \* $P < 0.05$ , \*\* $P < 0.001$  versus 0 μM of TET. **C.** The cell migration of HeLa and SiHa was detected by wound healing assay after treating with 10 μM of TET. **D.** The cell invasion ability of HeLa and SiHa was detected by transwell invasion assay after treating with 10 μM of TET. **E.** The epithelial-mesenchymal transition (EMT) related protein including E-cadherin and N-cadherin expression was detected by Western blotting after treating with TET in HeLa and SiHa. \*\* $P < 0.001$  versus DMSO group. C, x 100; D, x 250.

## miR-638 suppresses cervical cancer progression

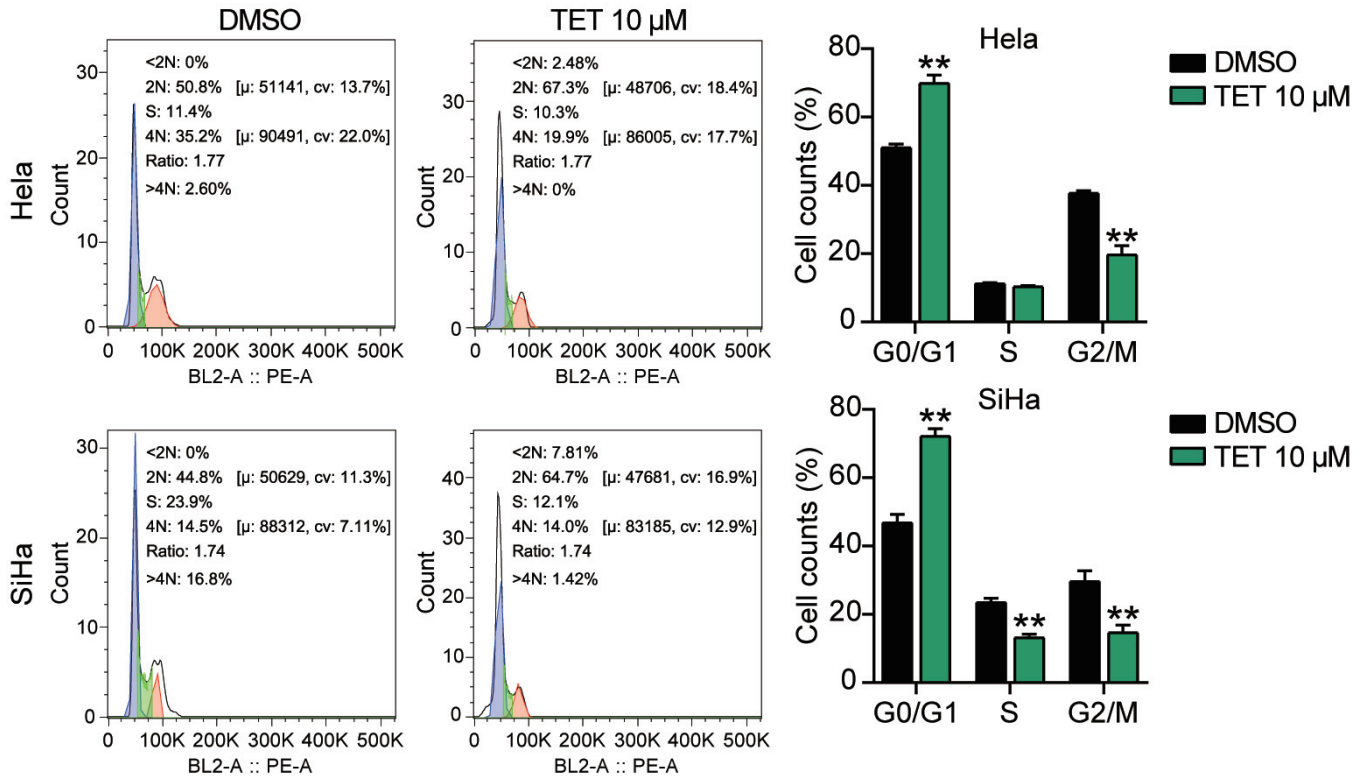


Fig. 2. The cell cycle HeLa and SiHa was detected by flow cytometry analysis after treating with 10 μM of TET. \*\*  $P < 0.001$  versus DMSO group.

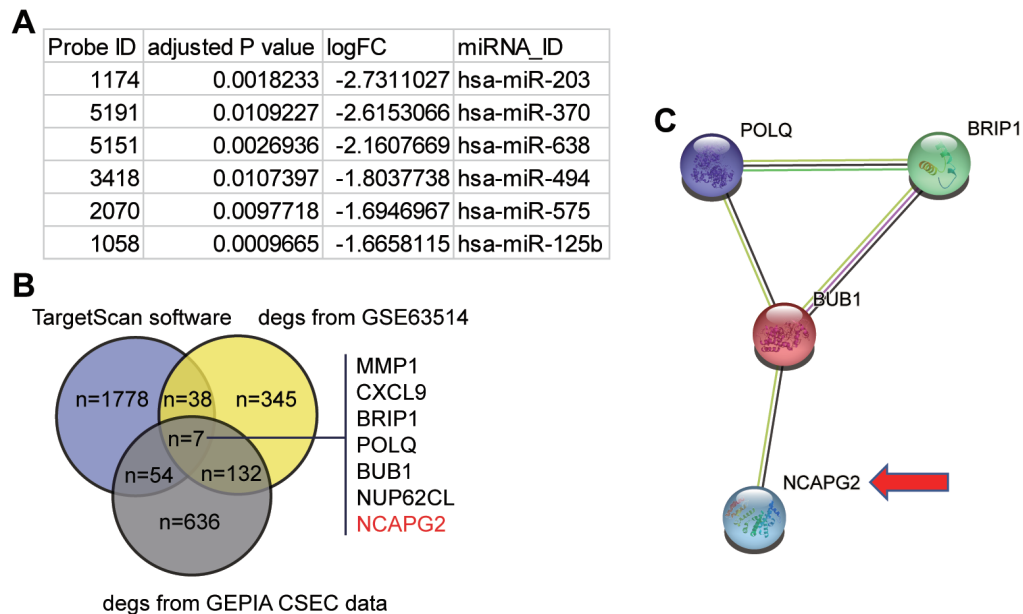
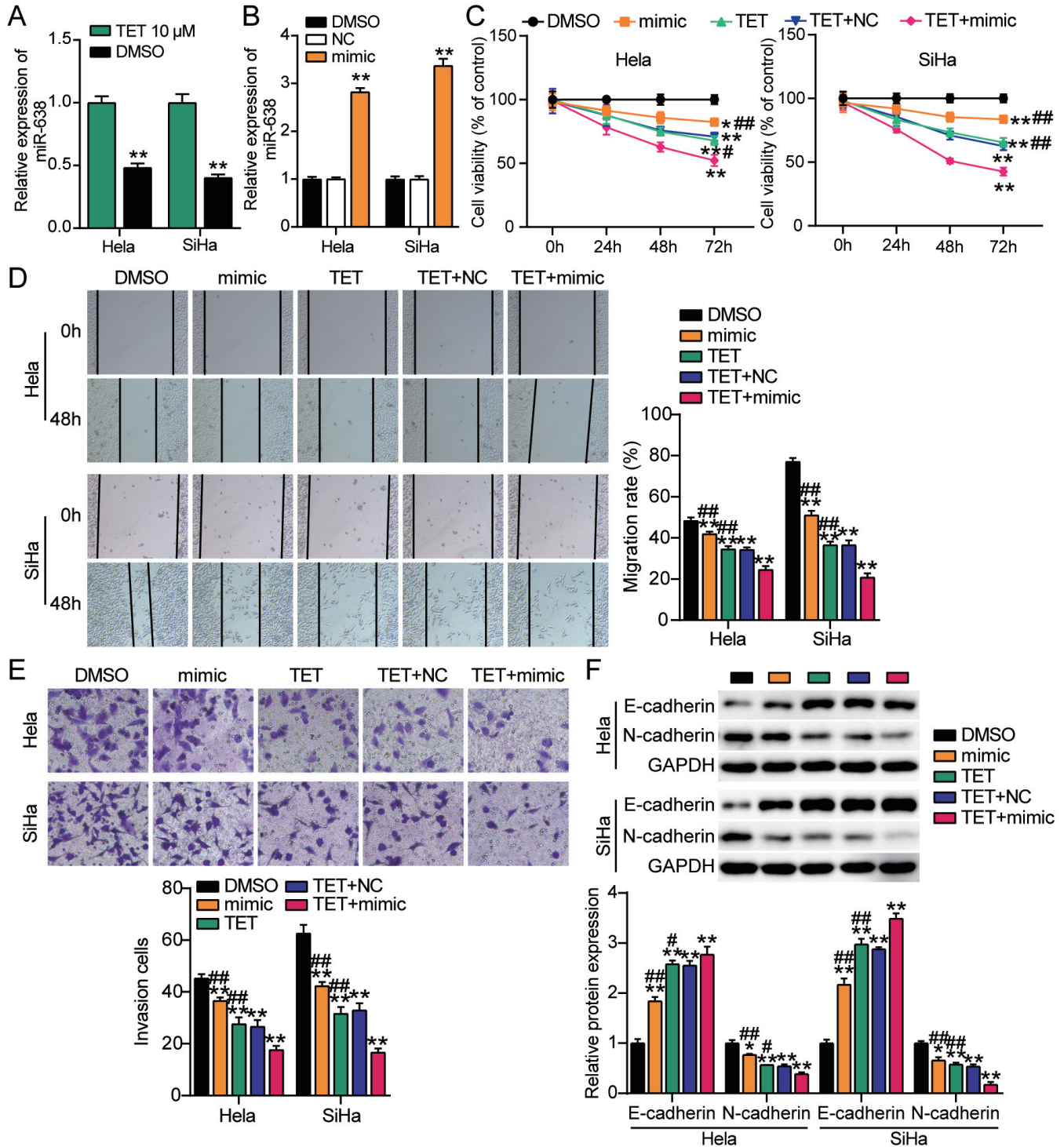


Fig. 3. miR-638 and NCAPG2 were selected as the study objects. **A**. The significantly differentially expressed miRNAs in CESC from GSE30656 analysis. CESC: cervical squamous cell carcinoma. FC: fold change. Gene selection criteria:  $\log_{2}FC \leq -1.5$  and adjusted  $P < 0.05$ . **B**. The intersection of the DEGs of GSE63514, DEGs of GEPIA CESC data, and the predicted targets of miR-638 by Targetscan. 7 genes were identified. The selection criteria for both GSE63514 and GEPIA CESC data were  $\log_{2}FC \geq 2$  and adjusted  $P < 0.05$ . **C**. The 7 gene PPI network analyzed by the STRING algorithm.

*miR-638 suppresses cervical cancer progression*



**Fig. 4.** miR-638 had an inhibitory impact on cervical cancer progress. **A.** miR-638 expression in HeLa and SiHa after treating with 10 μM of TET. \*\**P*<0.001 versus TMT 10μM group. **B.** The transfection effectiveness of miR-638 mimic in HeLa and SiHa. **C.** The synergistic effect of miR-638 and TET on HeLa and SiHa cell viability was found by CCK-8 assay. **D.** The synergistic effect of miR-638 and TET on HeLa and SiHa cell migration was detected by wound healing assay. **E.** The synergistic effect of miR-638 and TET on HeLa and SiHa cell invasion was identified by transwell invasion assay. **F.** The synergistic effect of miR-638 and TET on HeLa and SiHa cell E-cadherin and N-cadherin protein expression was detected by Western blotting. \**P*<0.05, \*\**P*<0.001 versus DMSO group, #*P*<0.05, ##*P*<0.001 versus TET+mimic group. D, x 100; E, x 200.

*miR-638 suppresses cervical cancer progression*

miR-638, hsa-miR-575, and hsa-miR-125b (Fig. 3A). We discovered that miR-638, which has previously been shown to reduce cervical cancer mobility phenotypes, was seldom explored in cervical cancer among these six miRNAs (Wei et al., 2017). We also obtained 522 and 829 differentially expressed genes (DEGs) from GSE63514 and GEPIA cervical cancer data, respectively. By intersecting the two datasets with the predicted targets of miR-638 using TargetScan, we obtained seven genes (Fig. 3B). The seven genes were then entered into the STRING, which was used to analyze protein-protein interactions. Four genes (*POLQ*, *BRIP1*, *BUB1*, and *NCAPG2*) were found to be tightly linked (Fig. 3C). Of these, *NCAPG2* is a key cancer driver in hepatocellular carcinoma (Meng et al., 2019) and lung cancer (Zhan et al., 2017). Nevertheless, the function of *NCAPG2* in cervical cancer has not been reported yet and is thus worth investigating. We speculated that miR-638 could suppress cervical cancer phenotypes by inhibiting *NCAPG2* expression.

*miR-638 had an inhibitory impact on cervical cancer progression*

When treated with 10  $\mu$ M TET, miR-638 expression

was twice as high as that in HeLa and SiHa cells treated only with DMSO (Fig. 4A), which suggested the combined inhibitory impact of miR-638 and TET in cervical cancer progression. To observe the influence of miR-638 on HeLa and SiHa cell development, miR-638 was successfully enriched by its mimic in these two cell lines, with about triple enrichment of expression (Fig. 4B). Cell viability was reduced by approximately 20% with overexpression of miR-638 in HeLa and SiHa cells, and this effect was even more remarkable when challenged with TET (Fig. 4C). Given that miR-638 exhibited a cell viability-repressive effect on cervical cancer cells, we continued to pay attention to the potential effect of miR-638 on the migration and invasion of HeLa and SiHa cells. As expected, miR-638 overexpression exerted a remarkable suppressive effect on SiHa and HeLa cell migration. Specifically, cell migration was reduced by 20 and 35%, respectively, in HeLa and SiHa cells treated with the miR-638 mimic, which became more significant due to the mutual effect of TET, leading to an approximate reduction of 50 and 70%, respectively (Fig. 4D). In addition, miR-638 showed a similar impact on HeLa and SiHa cell invasion. It was observed that cell invasion was dramatically repressed by approximately 20 and 35%,

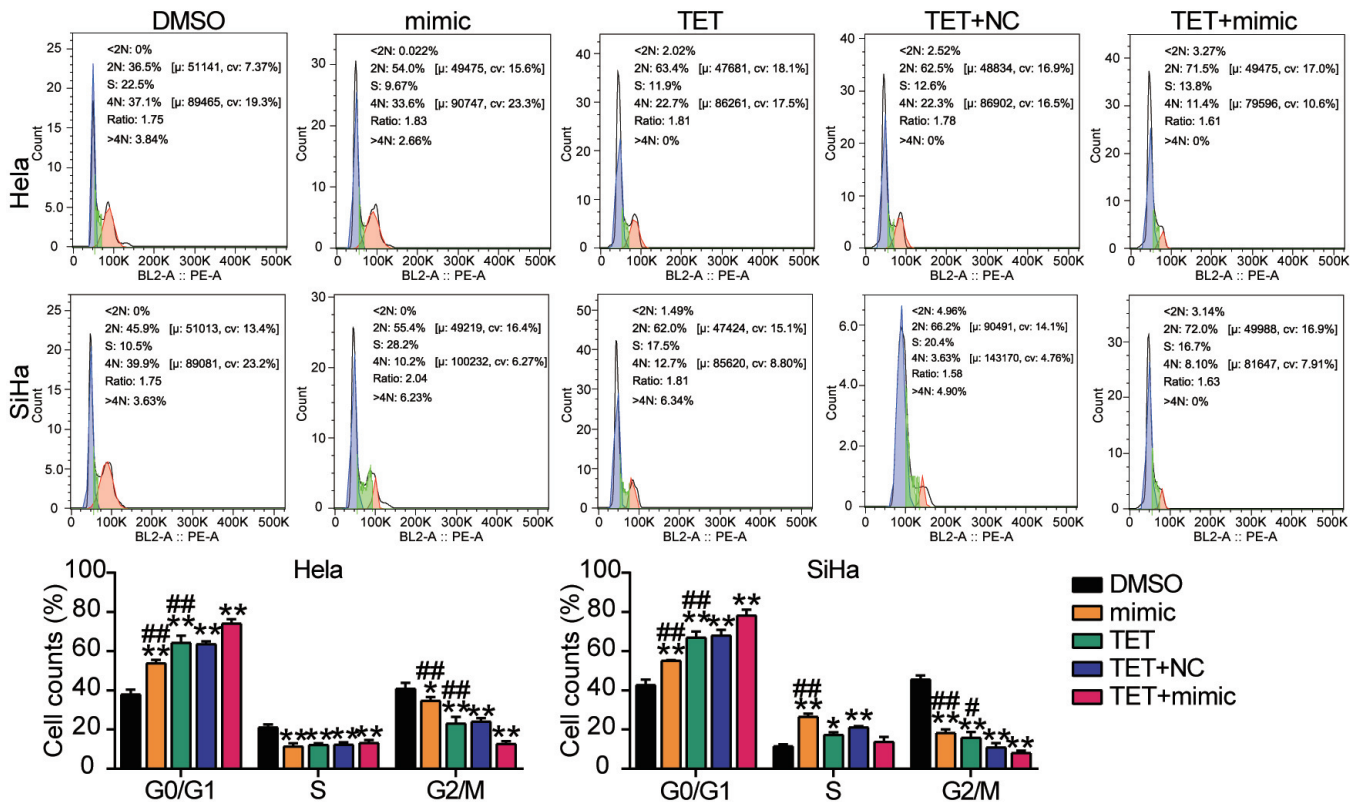
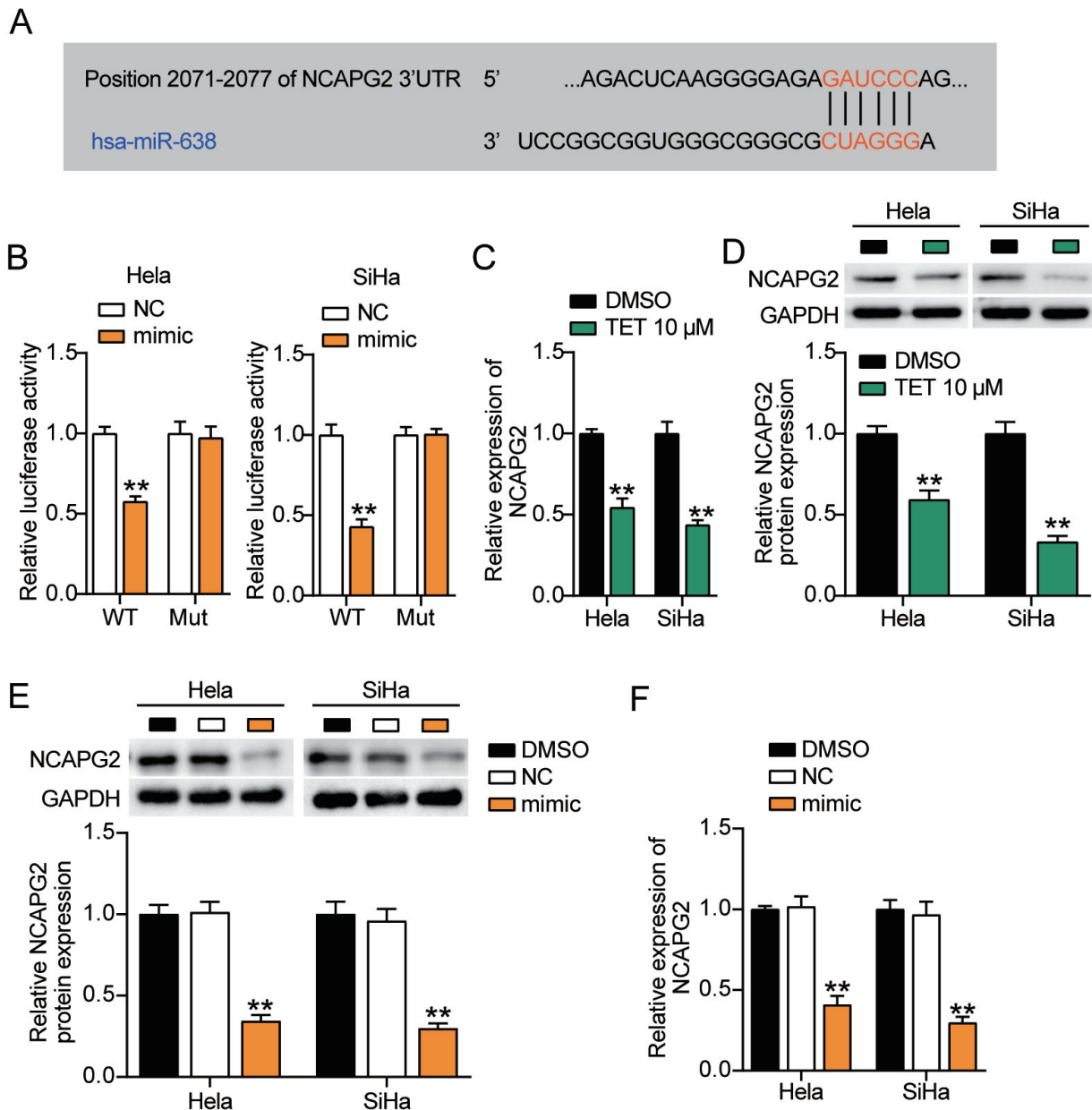


Fig. 5. The synergistic effect of miR-638 and TET on HeLa and SiHa cell cycle was identified by flow cytometry analysis. \* $P < 0.05$ , \*\* $P < 0.001$  versus DMSO group, # $P < 0.05$ , ## $P < 0.001$  versus TET+mimic group.

respectively, in HeLa and SiHa cells in the miR-638 mimic group, and this repression could also be enhanced by the synergy of TET, resulting in a repression of more than 60% (Fig. 4E). Additionally, evaluation of EMT components showed that miR-638 overexpression upregulated E-cadherin in HeLa and SiHa cells by 3.1 and 3.7 times, and decreased N-cadherin by 40 and 30%,

respectively. Co-treatment with TET and miR-638 mimic enhanced the inhibition of EMT, resulting in continued upregulation of E-cadherin by 1.8 and 1.6 times, as well as downregulation of N-cadherin by 75 and 70% in SiHa and HeLa cells (Fig. 4F). Moreover, miR-638 overexpression increased the proportion of G0/G1 phase cells and decreased the proportion of S



**Fig. 6.** NCAPG2 was a target gene of miR-638. **A.** The target relationship between miR-638 and NCAPG2 was predicted. **B.** The target association among miR-638 and NCAPG2 was validated by dual-luciferase assay in HeLa and SiHa. \*\* $P < 0.001$  versus NC group. **C.** NCAPG2 mRNA expression was detected by qRT-PCR after treating with TET in HeLa and SiHa. **D.** After TET treatment, Western blotting was used to determine NCAPG2 protein expression in HeLa and SiHa cells. **E.** NCAPG2 protein expression was detected by Western blotting after treating with miR-638 mimic in HeLa and SiHa. **F.** NCAPG2 mRNA expression was detected by qRT-PCR after treating with miR-638 mimic in HeLa and SiHa. (C-F) \*\* $P < 0.001$  versus DMSO group.

*miR-638 suppresses cervical cancer progression*

phase cells, and combined treatment with TET and miR-638 mimic further increased cell cycle arrest (Fig. 5). Overall, miR-638 slowed cervical cancer progression by inhibiting cell viability, migration, and invasion, which was aided by its interaction with TET.

*NCAPG2 was a target gene of miR-638*

To further understand the role of miR-638, TargetScan was used to determine its target gene. *NCAPG2* was predicted to be a target gene of miR-638

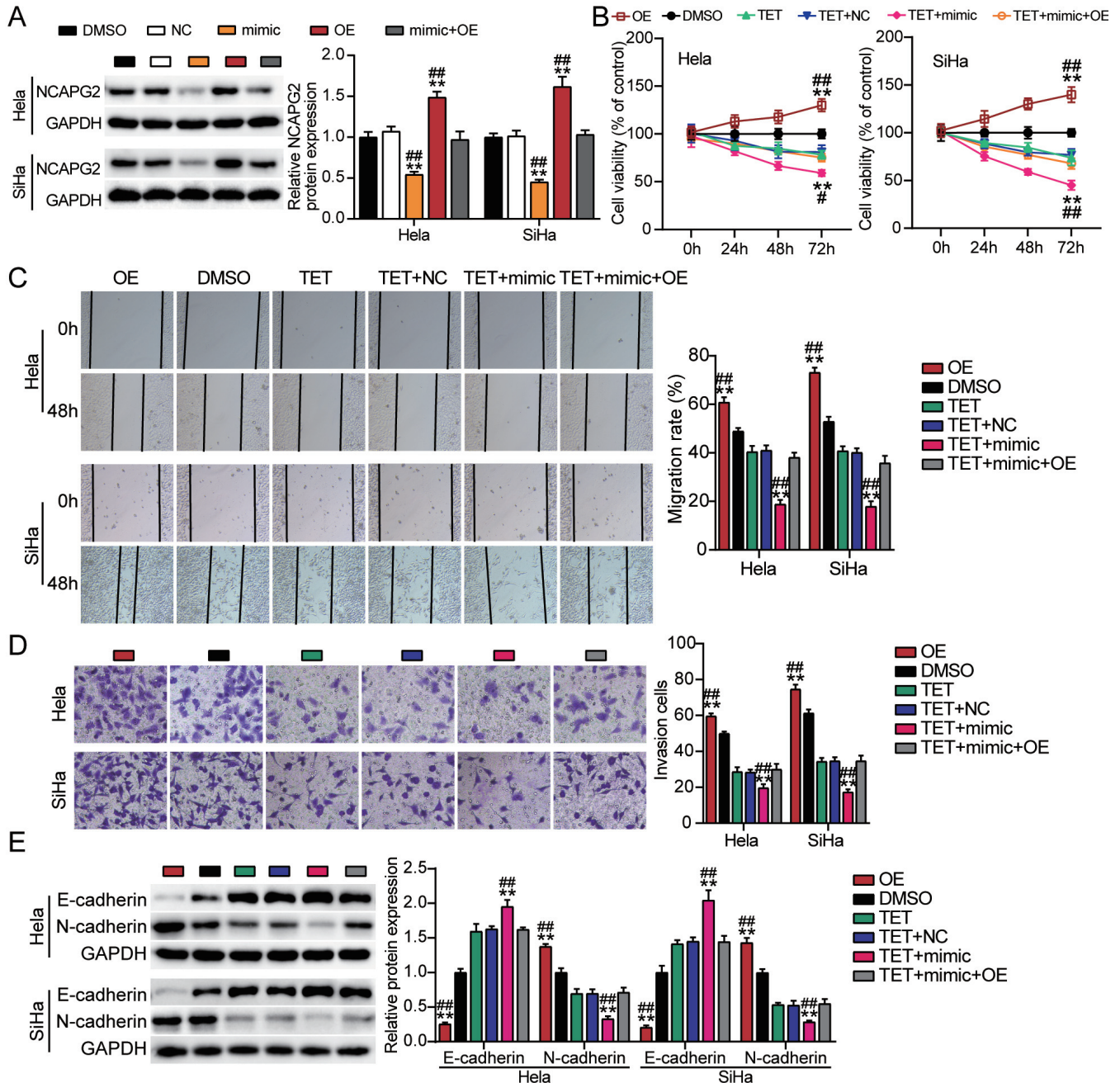


**Fig. 7.** The role of NCAPG2 in cervical cancer progress. **A.** NCAPG2 protein expression was observed by Western blotting after treating with miR-638 mimic or NCAPG2 overexpression in HeLa and SiHa.  $^{**}P<0.001$  versus DMSO group,  $^{\#}P<0.05$ ,  $^{\#\#}P<0.001$  versus mimic+OE group. **B.** The cell viability inhibition of miR-638 in HeLa and SiHa treated with TET was released by NCAPG2 overexpression. **C.** The cell migration inhibition of miR-638 in HeLa and SiHa treated with TET was released by NCAPG2 overexpression. **D.** The cell invasion inhibition of miR-638 in HeLa and SiHa treated with TET was released by NCAPG2 overexpression. **E.** The E-cadherin and N-cadherin protein expression of miR-638 in HeLa and SiHa treated with TET was affected by NCAPG2 overexpression. (B-E)  $^{**}P<0.001$  versus DMSO group,  $^{\#\#}P<0.001$  versus TET+mimic+OE group. C, x 200; D, x 200.

### miR-638 suppresses cervical cancer progression

in cervical cancer development using TargetScan, and the predicted binding site was position 2071-2076 of *NCAPG2* 3'-UTR (Fig. 6A). miR-638 mimic and *NCAPG2* WT led to a pronounced reduction in luciferase activity (approximately 50%), while no suppression of luciferase activity was observed in the mutant group, suggesting a direct binding of miR-638 to *NCAPG2* (Fig. 6B). Figure 6C illustrates that treatment with 10  $\mu$ M TET resulted in the reduction in *NCAPG2* mRNA expression by approximately 50% in HeLa and SiHa cells. In addition to the reduction in mRNA expression, there was also a 50 and 60% reduction in the protein expression of *NCAPG2* in TET-treated HeLa and SiHa cells, respectively (Fig. 6D). Furthermore, we investigated the changes in *NCAPG2* expression after overexpression of miR-63. Approximately, 35 and 50% reduction of *NCAPG2* protein levels, as well as 60 and 70% repression of mRNA expression were observed in HeLa and SiHa cells treated with miR-638 mimic, respectively (Fig. 6E,F). Taken together, we concluded that *NCAPG2* is a target gene of miR-638.

#### The role of *NCAPG2* in cervical cancer progression

Since *NCAPG2* has been shown to be a miR-638 target gene in the progression of cervical cancer, we further attempted to illustrate the consequence of *NCAPG2* on the development of SiHa and HeLa cells. We investigated the changes in *NCAPG2* protein expression after overexpression of miR-638 and

*NCAPG2*. *NCAPG2* protein levels in HeLa and SiHa cells increased by 1.4- and 1.7-fold, respectively, after *NCAPG2* overexpression (Fig. 7A). Moreover, *NCAPG2* overexpression almost completely reversed the effect of the miR-638 mimic on *NCAPG2* protein expression (Fig. 7A). We found that *NCAPG2* overexpression dramatically boosted the viability of HeLa and SiHa cells by more than 1.5-fold, but this enhancement was repressed by the synergistic action of miR-638 mimic and TET, resulting in a repression of more than 25% (Fig. 7B). Similarly, we also focused on the function of *NCAPG2* in invasion and migration of HeLa and SiHa cells. It was shown that *NCAPG2* overexpression promoted cell migration significantly by 1.2 and 1.4 times in HeLa and SiHa cells, respectively, while the promotion was inhibited by the co-existence of miR-638 and TET, leading to a reduction of approximately 25% (Fig. 7C). *NCAPG2* overexpression also facilitated cell invasion by 1.2-fold. Furthermore, *NCAPG2* overexpression-induced facilitation was suppressed by the orchestration of miR-638 and TET, resulting in a reduction of more than 50% (Fig. 7D). In addition, western blotting revealed a 60 and 50% decrease in E-cadherin protein levels and a 1.3- and 1.2-fold increase in N-cadherin protein levels caused by upregulation of *NCAPG2* in HeLa and SiHa cells, respectively. However, the co-existence of miR-638 and TET inhibited this effect (Fig. 7E). Flow cytometry analysis showed that overexpression of *NCAPG2* inhibited cell cycle arrest,

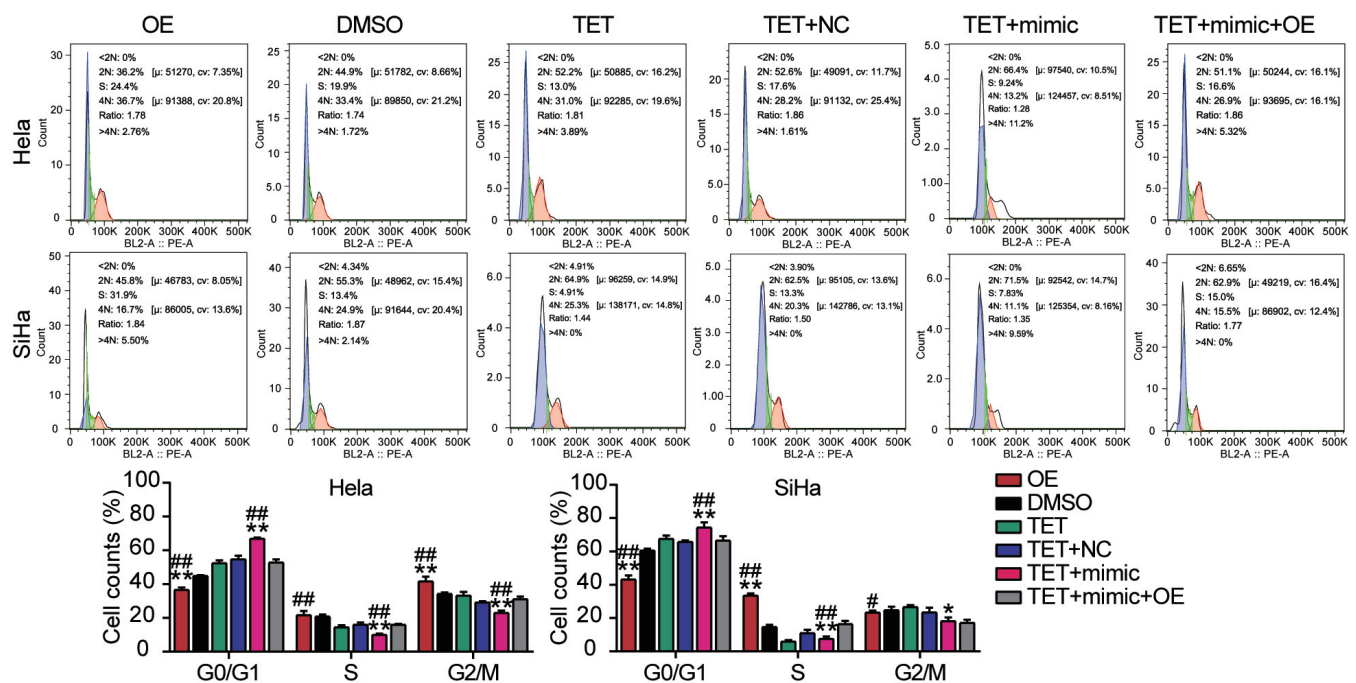


**Fig. 8.** The cell cycle arrest of miR-638 in HeLa and SiHa treated with TET was released by *NCAPG2* overexpression. \*\* $P < 0.001$  versus DMSO group, ## $P < 0.001$  versus TET+mimic+OE group.

## miR-638 suppresses cervical cancer progression

while TET and miR-638 reversed it (Fig. 8). Therefore, *NCAPG2* not only had a facilitating effect on cell migration but also on cell invasion, and all these effects were repressed by the interaction of miR-638 and TET.

### Discussion

In most cases, the incidence of cervical cancer is preventable by prophylactic HPV vaccinations as well as periodic surveillance via Pap smear-based testing and hrHPV (Burd, 2003; Moore, 2006). Unfortunately, HPV vaccines do not provide protection for people with stable existing infections. Thus, to better overcome the threat of cervical cancer occurrence, more advances, such as the discovery and application of novel biomarkers, are necessary. In this study, we explored potential new biomarkers for the development of cervical cancer. Specifically, using a TET-treated cell model, we identified that miR-638 is a cervical cancer-related miRNA that represses SiHa and HeLa cell viability, migration, invasion, and EMT. Moreover, *NCAPG2* was identified as a direct target gene of miR-638, exerting an opposite effect on the growth and development of SiHa and HeLa cells.

Infection of hrHPV into the cervical epithelium leads to host genome alterations, which include the silencing of multiple tumor suppressors and the dynamics of various pro-tumor factors (Srinivasan, 2019). Therefore, attempts to reveal these risk factors are of great value, as they will shed light on host-virus interactions on the one hand, and a better understanding of cervical tumorigenesis on the other. In this study, miR-638 was found to be a tumor suppressor in cervical cancer progression. A previous study applied qRT-PCR to measure serum expression levels of five miRNAs in cervical cancer patients and healthy individuals, and found that serum miR-638, miR-203a-3p, miR-1914-5p, and miR-521 levels were significantly reduced in the patient group, suggesting that miR-638 had an independent screening value (Zheng et al., 2020). Another study has shown that miR-638 expression has been reduced in tissue and cell lines of cervical cancer. (Wei et al., 2017). Furthermore, lower miR-638 expression was significantly associated with poor overall survival (Wei et al., 2017). Consistent with these data, our findings also revealed that miR-638 is downregulated in cervical cancer. Furthermore, an *in vitro* assay in the previous study (Wei et al., 2017) exhibited that miR-638 suppressed cell migration and invasion of HeLa cells, which was also in line with our results that miR-638 inhibited the migration and invasion of HeLa and SiHa cells.

To the best of our knowledge, this is the first study to demonstrate the role of miR-638/*NCAPG2* in cervical cancer progression. Previously, the tumor-promoting effect of *NCAPG2* has been reported in the pathogenesis of different cancers. For instance, a functional annotation

study of expression profiles associated with melanoma development revealed that *NCAPG2* was strongly linked to the upregulation of cell cycle activators (Ryu et al., 2007). *NCAPG2* promoted tumor progression via controlling the G2/M phase, and *NCAPG2* with high expression was linked to a poor prognosis in lung adenocarcinoma a decade later (Zhan et al., 2017). More recently, *NCAPG2* was indicated as an oncogene that contributes to hepatocellular carcinoma proliferation and metastasis by enriching interleukin (IL)-6 secretion (Meng et al., 2019). Our results are consistent with these previous reports, revealing a cervical cancer-promoting function of *NCAPG2*.

TET has been long used against cancer and has been reportedly applied as an anti-cancer agent in cancer chemotherapy as early as the beginning of the 21st century (Liu et al., 2003). In the last decade, emerging studies have indicated that TET plays a cancer-preventing role. For example, TET has an inhibitory effect on DNA synthesis and cell proliferation in laryngeal cancer stem cells (Cui et al., 2019). TET has also been shown to inhibit lung cancer development and cause apoptosis (Chen et al., 2018). In cervical cancer, TET can inhibit the proliferation, migration and invasion of cervical cancer cells *in vitro* and *in vivo* (Wang et al., 2019; Zhang et al., 2019). In addition, the effects of TET in combination with miRNA on disease development have also been reported. For example, TET promotes the expression of Occludin through the miR-429 pathway, thereby alleviating intestinal epithelial barrier defects caused by colitis (Chu et al., 2021). TET reduces myocardial infarction size by inhibiting miR-202-5p and promoting TRPV2 expression (Zhao et al., 2021). As a result, it makes sense to investigate the roles of miR-638 and *NCAPG2* in the development of cervical cancer in TET patients. TET decreased the vitality, migration, and invasion of HeLa and SiHa cells, according to our findings.

We have systematically characterized that miR-638 binds to *NCAPG2* and inhibits HeLa and SiHa cell viability, migration, invasion, and EMT in a TET-treated cell model. However, this study lacks *in vivo* experiments, which could be carried out in the future and provide more supportive evidence that miR-638/*NCAPG2* is an essential axis involved in cervical cancer development.

### Conclusion

This study demonstrated that miR-638 acts as a tumor suppressor in cervical cancer by repressing the viability, migration, invasion, and EMT of HeLa and SiHa cells. In addition, *NCAPG2* was discovered to be a miR-638 target gene and to have a role in cervical cancer development that is antagonistic to miR-638. Thus, miR-638 is a potential biomarker for cervical cancer diagnosis, as well as a predictor of cervical cancer prognosis.

**Acknowledgements.** None.

**Funding.** This work was supported by Natural Science Foundation of Hubei Province (grant number 2016CFB222).

**Conflicts of interest.** There are no conflicts of interest declared by the authors.

**Availability of data and material.** All data generated or analyzed during this study are included in this article.

**Code availability.** Not available.

**Authors contributions.** The tests and data analysis were carried out by MW and HZG. The research was planned and designed by HZG and ZMZ. The data was collected by HZG and KL. KL was in charge of data processing and interpretation. MW, HZG and KL wrote the paper. The article was reviewed and approved by all authors.

## References

- Agarwal V., Bell G.W., Nam J.W. and Bartel D.P. (2015). Predicting effective microRNA target sites in mammalian mRNAs. *Elife* 4, e05005.
- Bhagya N. and Chandrashekar K.R. (2018). Tetrandrone and cancer - An overview on the molecular approach. *Biomed. Pharmacother.* 97, 624-632.
- Burd E.M. (2003). Human papillomavirus and cervical cancer. *Clin. Microbiol. Rev* 16, 1-17.
- Chen Y.J. (2002). Potential role of tetrandrone in cancer therapy. *Acta Pharmacol. Sin.* 23, 1102-1106.
- Chen Z., Zhao L., Zhao F., Yang G. and Wang J.J. (2018). Tetrandrone suppresses lung cancer growth and induces apoptosis, potentially via the VEGF/HIF-1 $\alpha$ /ICAM-1 signaling pathway. *Oncol. Lett.* 15, 7433-7437.
- Chow L.W.C., Cheng K.S., Leong F., Cheung C.W., Shiao L.R., Leung Y.M. and Wong K.L. (2019). Enhancing tetrandrone cytotoxicity in human lung carcinoma A549 cells by suppressing mitochondrial ATP production. *Naunyn. Schmiedeberg's. Arch. Pharmacol.* 392, 427-436.
- Chu Y., Zhu Y., Zhang Y., Liu X., Guo Y., Chang L., Yun X., Wei Z., Xia Y. and Dai Y. (2021). Tetrandrone attenuates intestinal epithelial barrier defects caused by colitis through promoting the expression of occludin via the AhR-miR-429 pathway. *FASEB J.* 35, e21502.
- Cui X., Xiao D. and Wang X. (2019). Inhibition of laryngeal cancer stem cells by tetrandrone. *Anticancer Drugs* 30, 886-891.
- den Boon J.A., Pyeon D., Wang S.S., Horswill M., Schiffman M., Sherman M., Zuna R.E., Wang Z., Hewitt S.M., Pearson R., Schott M., Chung L., He Q., Lambert P., Walker J., Newton M.A., Wentzensen N. and Ahlquist P. (2015). Molecular transitions from papillomavirus infection to cervical precancer and cancer: Role of stromal estrogen receptor signaling. *Proc. Natl. Acad. Sci. USA* 112, E3255-3264.
- Fang J., Zhang H. and Jin S. (2014). Epigenetics and cervical cancer: From pathogenesis to therapy. *Tumour Biol.* 35, 5083-5093.
- Khan T.N., Khan K., Sadeghpour A., Reynolds H., Perilla Y., McDonald M.T., Gallentine W.B., Baig S.M., Davis E.E. and Katsanis N. (2019). Mutations in NCAPG2 cause a severe neurodevelopmental syndrome that expands the phenotypic spectrum of condensinopathies. *Am. J. Hum. Genet.* 104, 94-111.
- Kuroda H., Nakazawa S., Katagiri K., Shiratori O. and Kozuka M. (1976). Antitumor effect of bisbenzylisoquinoline alkaloids. *Chem. Pharm. Bull (Tokyo)* 24, 2413-2420.
- Kwan C.Y. and Achike F.I. (2002). Tetrandrone and related bisbenzylisoquinoline alkaloids from medicinal herbs: Cardiovascular effects and mechanisms of action. *Acta Pharmacol. Sin.* 23, 1057-1068.
- Laengsri V., Kerdpin U., Plabplueng C., Treeratanapiboon L. and Nuchnoi P. (2018). Cervical cancer markers: Epigenetics and microRNAs. *Lab. Med.* 49, 97-111.
- Liao D., Zhang W., Gupta P., Lei Z.N., Wang J.Q., Cai C.Y., Vera A.A., Zhang L., Chen Z.S. and Yang D.H. (2019). Tetrandrone interaction with ABCB1 reverses multidrug resistance in cancer cells through competition with anti-cancer drugs followed by downregulation of ABCB1 expression. *Molecules* 24, 4383.
- Liu Z.L., Hirano T., Tanaka S., Onda K. and Oka K. (2003). Persistent reversal of P-glycoprotein-mediated daunorubicin resistance by tetrandrone in multidrug-resistant human T lymphoblastoid leukemia MOLT-4 cells. *J. Pharm. Pharmacol.* 55, 1531-1537.
- Meng F., Zhang S., Song R., Liu Y., Wang J., Liang Y., Wang J., Han J., Song X., Lu Z., Yang G., Pan S., Li X., Liu Y., Zhou F., Wang Y., Cui Y., Zhang B., Ma K., Zhang C., Sun Y., Xin M. and Liu L. (2019). NCAPG2 overexpression promotes hepatocellular carcinoma proliferation and metastasis through activating the STAT3 and NF- $\kappa$ B/miR-188-3p pathways. *EBioMedicine* 44, 237-249.
- Moore D.H. (2006). Cervical cancer. *Obstet. Gynecol.* 107, 1152-1161.
- Mori M.A., Ludwig R.G., Garcia-Martin R., Brandão B.B. and Kahn C.R. (2019). Extracellular miRNAs: From biomarkers to mediators of physiology and disease. *Cell. Metab.* 30, 656-673.
- Olusola P., Banerjee H.N., Phillely J.V. and Dasgupta S. (2019). Human papilloma virus-associated cervical cancer and health disparities. *Cells* 8, 622.
- Pardini B., De Maria D., Francavilla A., Di Gaetano C., Ronco G. and Naccarati A. (2018). MicroRNAs as markers of progression in cervical cancer: A systematic review. *BMC Cancer* 18, 696.
- Park S., Eom K., Kim J., Bang H., Wang H.Y., Ahn S., Kim G., Jang H., Kim S., Lee D., Park K.H. and Lee H. (2017). MiR-9, miR-21, and miR-155 as potential biomarkers for HPV positive and negative cervical cancer. *BMC Cancer* 17, 658.
- Rao M.R. (2002). Effects of tetrandrone on cardiac and vascular remodeling. *Acta Pharmacol. Sin.* 23, 1075-1085.
- Ryu B., Kim D.S., Deluca A.M. and Alani R.M. (2007). Comprehensive expression profiling of tumor cell lines identifies molecular signatures of melanoma progression. *PLoS One* 2, e594.
- Sadri Nahand J., Moghoofei M., Salmaninejad A., Bahmanpour Z., Karimzadeh M., Nasiri M., Mirzaei H.R., Pourhanifeh M.H., Bokharaei-Salim F., Mirzaei H. and Hamblin M.R. (2020). Pathogenic role of exosomes and microRNAs in HPV-mediated inflammation and cervical cancer: A review. *Int. J. Cancer* 146, 305-320.
- Shishodia G., Shukla S., Srivastava Y., Masaldan S., Mehta S., Bhamhani S., Sharma S., Mehrotra R., Das B.C. and Bharti A.C. (2015). Alterations in microRNAs miR-21 and let-7a correlate with aberrant STAT3 signaling and downstream effects during cervical carcinogenesis. *Mol. Cancer* 14, 116.
- Srinivasan R. (2019). Cervical cancer genomics: An initial step towards personalized approach to therapy. *EBioMedicine* 43, 11-12.
- Sun Q., Yang Z., Li P., Wang X., Sun L., Wang S., Liu M. and Tang H. (2019). A novel miRNA identified in GRSF1 complex drives the metastasis via the PIK3R3/AKT/NF- $\kappa$ B and TIMP3/MMP9 pathways in cervical cancer cells. *Cell Death Dis.* 10, 636.
- Thadani R., Uhlmann F. and Heeger S. (2012). Condensin, chromatin crossbarring and chromosome condensation. *Curr. Biol.* 22, R1012-

*miR-638 suppresses cervical cancer progression*

- 1021.
- Wang X., Chen Y., Li J., Guo S., Lin X., Zhang H., Zhan Y. and An H. (2019). Tetrandrine, a novel inhibitor of ether-à-go-go-1 (Eag1), targeted to cervical cancer development. *J. Cell. Physiol.* 234, 7161-7173.
- Wei H., Zhang J.J. and Tang Q.L. (2017). MiR-638 inhibits cervical cancer metastasis through Wnt/ $\beta$ -catenin signaling pathway and correlates with prognosis of cervical cancer patients. *Eur. Rev. Med. Pharmacol. Sci.* 21, 5587-5593.
- Wiltling S.M., van Boerdonk R.A., Henken F.E., Meijer C.J., Diosdado B., Meijer G.A., le Sage C., Agami R., Snijders P.J. and Steenbergen R.D. (2010). Methylation-mediated silencing and tumour suppressive function of hsa-miR-124 in cervical cancer. *Mol. Cancer* 9, 167.
- Wiltling S.M., Snijders P.J., Verlaet W., Jaspers A., van de Wiel M.A., van Wieringen W.N., Meijer G.A., Kenter G.G., Yi Y., le Sage C., Agami R., Meijer C.J. and Steenbergen R.D. (2013). Altered microRNA expression associated with chromosomal changes contributes to cervical carcinogenesis. *Oncogene* 32, 106-116.
- Yao W.X. and Jiang M.X. (2002). Effects of tetrandrine on cardiovascular electrophysiologic properties. *Acta Pharmacol. Sin.* 23, 1069-1074.
- Zhan P., Xi G.M., Zhang B., Wu Y., Liu H.B., Liu Y.F., Xu W.J., Zhu Q., Cai F., Zhou Z.J., Miu Y.Y., Wang X.X., Jin J.J., Li Q., Lv T.F. and Song Y. (2017). NCAPG2 promotes tumour proliferation by regulating G2/M phase and associates with poor prognosis in lung adenocarcinoma. *J. Cell. Mol. Med.* 21, 665-676.
- Zhang J., Bian Z., Zhou J., Song M., Liu Z., Feng Y., Zhe L., Zhang B., Yin Y. and Huang Z. (2015). MicroRNA-638 inhibits cell proliferation by targeting phospholipase D1 in human gastric carcinoma. *Protein Cell* 6, 680-688.
- Zhang T.J., Guo R.X., Li X., Wang Y.W. and Li Y.J. (2017). Tetrandrine cardioprotection in ischemia-reperfusion (I/R) injury via JAK3/STAT3/Hexokinase II. *Eur. J. Pharmacol.* 813, 153-160.
- Zhang H., Xie B., Zhang Z., Sheng X. and Zhang S. (2019). Tetrandrine suppresses cervical cancer growth by inducing apoptosis *in vitro* and *in vivo*. *Drug. Des. Devel. Ther.* 13, 119-127.
- Zhao W., Wu Y., Ye F., Huang S., Chen H., Zhou R. and Jiang W. (2021). Tetrandrine ameliorates myocardial ischemia reperfusion injury through miR-202-5p/TRPV2. *Biomed. Res. Int.* 2021, 8870674.
- Zheng D.H., Wang X., Lu L.N., Chen D.L., Chen J.M., Lin F.M. and Xu X.B. (2018). MiR-638 serves as a tumor suppressor by targeting HOXA9 in glioma. *Eur. Rev. Med. Pharmacol. Sci.* 22, 7798-7806.
- Zheng S., Li R., Liang J., Wen Z., Huang X., Du X., Dong S., Zhu K., Chen X., Liu D., Wu J., Liu Y., Zou X., Wang Y., Li J., Zeng F., Feng L., Yang G. and Jing C. (2020). Serum miR-638 combined with squamous cell carcinoma-related antigen as potential screening biomarkers for cervical squamous cell carcinoma. *Genet. Test. Mol. Biomarkers* 24, 188-194.
- Zhou X., Chen J., Xiao Q., Wang T., Yu Y., Li B., Shao G., Li Y. and Zhang Z. (2018). MicroRNA-638 inhibits cell growth and tubule formation by suppressing VEGFA expression in human ewing sarcoma cells. *Biosci. Rep.* 38, BSR20171017.

Accepted August 4, 2023